resources

MDPI

Article

The Environmental Oxidation of Acetaminophen in Aqueous Media as an Emerging Pharmaceutical Pollutant Using a Chitosan Waste-Based Magnetite Nanocomposite

Manasik M. Nour [1,*] and Maha A. Tony [2,3,*]

[1] Department of Mathematics, College of Science and Humanities in Al-Kharj, Prince Sattam Bin Abdulaziz University, Al-Kharj 11942, Saudi Arabia
[2] Basic Engineering Science Department, Faculty of Engineering, Menoufia University, Shibin El-Kom 32511, Egypt
[3] Advanced Materials/Solar Energy and Environmental Sustainability (AMSEES) Laboratory, Faculty of Engineering, Menoufia University, Shibin El-Kom 32511, Egypt
* Correspondence: m.mohamednour@psau.edu.sa (M.M.N.); maha.shalaby@sh-eng.menofia.edu.eg or dr.maha.tony@gmail.com (M.A.T.)

Abstract: Clean water is a precious and limited resource that plays a crucial role in supporting life on our planet. However, the industrial sector, especially the pharmaceutical industry, significantly contributes to water consumption, and this can lead to water body pollution. Fenton's reagent was introduced in the current investigation to oxidize acetaminophen as an emerging pollutant in such effluents. Therefore, we employed a straightforward co-precipitation method to fabricate chitosan-coated magnetic iron oxide, which is referred to in this study as Chit@Fe_3O_4. X-ray diffraction spectroscopy (XRD), Fourier transform infrared (FTIR), diffuse reflectance spectra (DRS), scanning electron microscopy (TEM), and transmission electron microscopy (TEM) were utilized to characterize the sample. It is crucial to treat such effluents due to the rapid increase in emerging pollutants. In this study, a photo-Fenton system was introduced as a combination of a Chit@Fe_3O_4 catalyst augmented with hydrogen peroxide under ultraviolet (UV) illumination conditions. The results reveal that only 1 h of irradiance time is efficient in oxidizing acetaminophen molecules. Doses of 20 and 200 mg/L of Chit@Fe_3O_4 and H_2O_2, respectively, and a pH of 2.0 were recorded as the optimal operational conditions that correspondingly oxidize 20 mg/L of acetaminophen to a 95% removal rate. An increase in the reaction temperature results in a decline in the reaction rate, and this, in turn, confirms that the reaction system is exothermic in nature. The sustainability of the catalyst was verified and deemed adequate in treating and oxidizing acetaminophen, even up to the fourth cycle, achieving a 69% removal rate. A kinetic modeling approach is applied to the experimental results, and the kinetic data reveal that the oxidation system conforms to second-order kinetics, with rate constants ranging from 0.0157 to 0.0036 L/mg·min. Furthermore, an analysis of the thermodynamic parameters reveals that the reaction is exothermic and non-spontaneous, predicting an activation energy of 36.35 kJ/mol. Therefore, the proposed system can address the limitations associated with the homogeneous Fenton system.

Keywords: chitosan/magnetite nanocomposite; photocatalyst; pharmaceutical product; wastewater; acetaminophen

Citation: Nour, M.M.; Tony, M.A. The Environmental Oxidation of Acetaminophen in Aqueous Media as an Emerging Pharmaceutical Pollutant Using a Chitosan Waste-Based Magnetite Nanocomposite. *Resources* **2024**, *13*, 47. https://doi.org/10.3390/resources13030047

Academic Editor: Seong-Nam Nam

Received: 5 January 2024
Revised: 14 February 2024
Accepted: 19 February 2024
Published: 19 March 2024

1. Introduction

Approximately four thousand pharmaceutical products exist and are accessible on the market [1]. The release of such products into the environment is linked to industrial spills, hospital discharge, and domestic waste disposal, and these may be released through expired stock. Such discharge must be treated prior to disposal to conserve the plant [2,3]. Acetaminophen (N-(4-hydroxyphenyl) is one of the most accessible drugs in the market and

has been detected in both surface and underground waters in some countries [4]. However, its presence in aquaculture may cause severe damage to health, including hormone disruption, the inhibition of metabolic processes, and damage to the liver [5]. Acetaminophen, originally synthesized in the mid-19th century, is commonly known as paracetamol. It has gained extensive utilization as an easily accessible over-the-counter medication for fever, headache, and postoperative pain relief, serving as an antipyretic and analgesic remedy [2–4]. Acetaminophen has received extensive usage because of its significant therapeutic effectiveness and economic production expenses. A total of 50 tons of acetaminophen per million inhabitants is consumed annually, reaching a total consumption exceeding 149,300 tons worldwide [5]. However, about 50 to 70% of this product is released into the environment and damages aqueous systems. Acetaminophen has been detected in various ecosystems due to incomplete metabolism and mineralization processes, thus posing a serious threat to aquaculture and human health [6]. Therefore, it is vital to implement effective strategies are vital to prevent the persistent buildup of acetaminophen in natural water environments and mitigate its detrimental impacts on public health and ecosystems [7,8].

Conventional wastewater treatment plants do not sufficiently provide since they do not remove waste from water and also introduce problems, such as secondary wastes known as toxic metabolic intermediates [9]. Advanced oxidation processes (AOPs) are promising treatment methods for achieving the complete mineralization of wastewater. The Fenton reaction system is an AOP that is considered a significant and effective approach due to its several advantages which include its rapid high performance and complete degradation of organic compounds while producing environmentally friendly end products [10]. Due to their enhanced properties and effectiveness, the use of nanoscale photo-catalysts in pharmaceutically polluted wastewater elimination has recently gained the attention of researchers [11–13]. However, industrial-scale photocatalytic application techniques are still limited in the field [14]. In this regard, it is necessary to conduct further research to achieve more practical applications.

Over the last few decades, the remediation of emerging pollutants via the Fenton oxidation reaction revealed "Green" features, providing great advantages in terms of its harmless end-product reaction (involving CO_2 and H_2O), which is both harmless and results in complete mineralization [15,16]. This process is also considered a technology of viable economic value since its operating and maintenance costs are minimal compared to other traditional wastewater treatment technologies [17]. However, these limitations still hinder real-life applications [17]. For instance, sludge is produced following the reaction process conducted using a homogenous Fenton catalyst source, which is difficult to separate from reclaimed water, and this is a considerable disadvantage of this procedure. Thus, the Fenton catalyst source could be substituted with a heterogeneous candidate.

Therefore, recent advances in research have been applied to combat these limitations [18,19]. A classical Fenton reagent is classified in the literature as a type of homogenous Fenton technology, which comprises H_2O_2 and iron ions [20]. Iron is signified as the rate-limiting step in a catalytic cycle [21]. in H_2O_2 also presents some disadvantages, including its explosive and toxic qualities as well as the harm it poses on human health when consumed in a concentrated solution [22,23]. Furthermore, iron can be precipitated into Fe^{3+} in solutions with a pH level higher than 3.0, forming iron sludge [24]. Additionally, iron precipitate is difficult to separate from the medium, which is classified as one of the limitations of the classical Fenton system [25]. This drawback not only reduces the reaction rate, since it loses iron activity in the reaction, but also represents secondary pollutants. The research on various scenarios for achieving a viable Fenton's process cost is still in the works. A heterogeneous catalyst has been introduced to establish the leading research in this field and to overcome the disadvantages of using a homogenous Fenton system [26]. From this perspective, searching for an iron material as a supporting heterogeneous carrier is significant; for instance, previously, zeolite was applied as a Fenton support material [18]. Furthermore, other studies introduced oxalic acid augmented with an iron catalyst to prevent iron precipitation [19].

Chitosan is a natural polymer that possess good mechanical strength; it is also a harmless substance that is economically efficient, has high water permeability, and can chemical transform to become a nanocomposite subsequent to the addition of metal oxides [27–29]. Chitosan is extensively used in the field as an adsorbent material in the removal of pollutants from wastewater since it has hydroxyl and amino functional groups [30–33]. These functional groups could be protonated in acidic solution, generating considerable electrostatic attraction to anionic molecules. Nevertheless, according to the literature [34–38], its applications as a photocatalytic material remains limited. Additionally, although chitosan is an effective component for water treatment, the catalyst separation that occurs after treatment remains a difficult issue. Hence, to achieve better separation of pollutants from aqueous media after treatment, the combination of chitosan with magnetite nanoparticles is recommended, yielding an easy recoverable and recyclable catalyst. Thus, this composite is non-toxic and environmentally friendly. Currently, hybrid substances formed from chitosan and nanoparticles, such as metal–chitosan substances, are attracting more attention in research concerning the removal of toxic pollutants from aqueous media since they act as efficient adsorbents. In previous research, chitosan composites were augmented with carbon nanoparticles [39], with the use of chitosan/hematite as an adsorbent material [40] and chitosan impregnated with titanium dioxide as an adsorbent material for the purpose of toxic pollutant removal [41]. To illustrate this concept further, carbon nanoparticles augmented with chitosan were prepared using a one-step hydrothermal technique, and their fluorescence properties indicated the scavenging effect of chitosan/carbon nanoparticles for the removal of heavy metal ions from polluted wastewater. This composite can form a stable complexion wherein heavy metal ions are eliminated from the water via the process of sedimentation [39]. The thermal decomposition method was used to synthesize hematite-impregnated chitosan nanoparticles and applied as an antibacterial agent to investigate the antibacterial activity of magnetic nanoparticles [40]. Titanium-dioxide-impregnated chitosan beads were used to eliminate chromium heavy metal from wastewater through the photo-reduction technique [41]. However, according to the literature, this method has not been applied on a wide scale for oxidizing a pollutant as one of the Fenton's reagent oxidation tests in a photocatalytic reaction. It is worth mentioning that magnetic chitosan possesses valuable properties, including low costs, biodegradability, the capacity to be extracted from green sources, and high magnetic intensity. These characteristics of magnetic chitosan reveal the great potential of the catalyst as an economic and operationally beneficial material since it can be separated and sustained for successive use. Additionally, magnetic nanoparticles are superior when integrated with chitosan since they offer the benefits of the incorporation of the functional layer with chitosan, reducing aggregation and improving biocompatibility [39].

The aim of this work is to assess the feasibility of a chitosan polymer conjugate with Fe as an efficient hetro-junction composite and photocatalyst. The catalyst was used as a source of heterogamous Fenton reaction to assess the sustainability and environmental friendliness of this composite. This material is used for the elimination of acetaminophen, one of the most widely used anti-inflammatory drug [35]. However, it possesses high toxicity, high persistence, and carcinogenic effects. Acetaminophen appears after its disposal in domestic sewage and, thus, release into the environment, which might affect the usual behavior of active sludge. Thus, a composite of chitosan and magnetite is introduced herein as a heterogeneous novel photo-Fenton catalyst system for oxidizing acetaminophen from aqueous effluent. Furthermore, the system parameters were investigated to comprehensively evaluate the performance of the photocatalytic reaction. First, a magnetic chitosan photocatalyst was prepared; then, the structure and morphology were characterized and analyzed via X-ray diffraction (XRD), scanning electron microscopy (SEM), and transmission electron microscopy (TEM). Different catalyst and hydrogen peroxide dosages, initial acetaminophen concentrations, system pH values, and temperatures were applied, and the maximum removal performance was assessed. Also, thermodynamic and kinetic modeling were performed to assess potential practical applications. The recyclability of

this hetro-junction composite was also evaluated. Furthermore, the possible oxidation mechanism was proposed in this study.

2. Experimental Investigation

2.1. Chitosan-Magnetite Composite Preparation

Chitosan polymer augmented magnetite nanoparticles, Chit@Fe_3O_4 nanocomposite were synthesized via simple co-precipitation technique. This method was selected due to its various benefits, such as high yield, high product purity, and the lack of a need for organic solvents. This method offers significant advantages in terms of preparation and small particle size distribution [3]. The Chit@Fe_3O_4 sample is prepared via the co-precipitation technique followed by hydrothermal treatment [36]. Firstly, 1% wt. of chitosan powder (carboxymethyl chitosan, degree of deacetylation $\geq$ 90%, and molecular weight of 543.5) was dissolved in a few droplets of the CH_3COOH solution; then, 50 mL of distilled water was added while stirring. Next, ferrous sulfate and ferric chloride salts of a 1:2 molar ratio were individually dissolved in 50 mL of water. Subsequently, the three resulting solutions were combined, and hydroxide solution was added to elevate the pH of the mixture to 10. The mixture was then subjected to heating at 90 °C for one hour. Afterward, the resulting precipitate was washed with distilled water until a pH of 7.0 was achieved. Finally, the clean precipitate was dried overnight at 105 °C; thus, the catalyst was ready for use and labeled as Chit@Fe_3O_4. Therefore, the prepared sample was ready for the catalytic oxidation tests of acetaminophen in aqueous effluents.

2.2. Methodology

To begin, acetaminophen obtained from Sigma Aldrich was utilized as the source of synthetic pharmaceutical effluent. Acetaminophen powder was directly used without any additional treatment or purification. A stock solution of 1000 mg/L from acetaminophen was prepared and then subjected to successive dilutions to obtain the required concentration. The prepared acetaminophen concentration was then subjected to treatment.

Then, 100 mL of acetaminophen aqueous effluent was transferred to a glass vessel, and the initial pH of the solution was adjusted as necessary. For pH adjustment, a digital pH meter (model AD1030, Adwa instrument, Szeged, Hungary) was employed, and diluted H_2SO_4 and/or NaOH solutions were applied to attain the required concentration. Subsequently, the Chit@Fe_3O_4 catalyst was added to the solution, and then the mixture is subjected to ultrasonic vibration for 5 min to assure catalyst dispersion. Afterward, the Fenton reaction was initiated using hydrogen peroxide (30% w/v). Furthermore, the operating parameters were investigated, such as hydrogen peroxide (ranged from 50 to 400 mg/L), Chit@Fe_3O_4 in the range of (5 to 100 mg/L), and pH value 2–6, while the acetaminophen concentration ranged from 20 to 100 mg/L. Additionally, the temperature was changed from room temperature (26 °C) to 60 °C to investigate its effect. To check the significance of each parameter, a one-factor-at-a-time factor effect analysis was applied by changing the range of each parameter while keeping the other factors constant. Then, the solution containing acetaminophen and reagents was exposed to ultraviolet illumination through a sleeved jacked (UV lamp, 15 W, with 253.7 nm) to introduce the photo-oxidation reaction. Then, after treatment, the samples were subjected to analysis. Accordingly, the samples were filtered through a microfilter (0.45 µm) and then subjected to periodic analysis through spectrophotometric analysis at the maximum wavelength of acetaminophen (243 nm). The analysis was conducted using a visible spectrophotometer (Unico UV-2100, Peabody, MA, USA). The analysis was conducted in three replicates for all experiments, and the data displayed are the average value. The graphical illustration of the experimental set-up and treatment steps is shown in Figure 1.

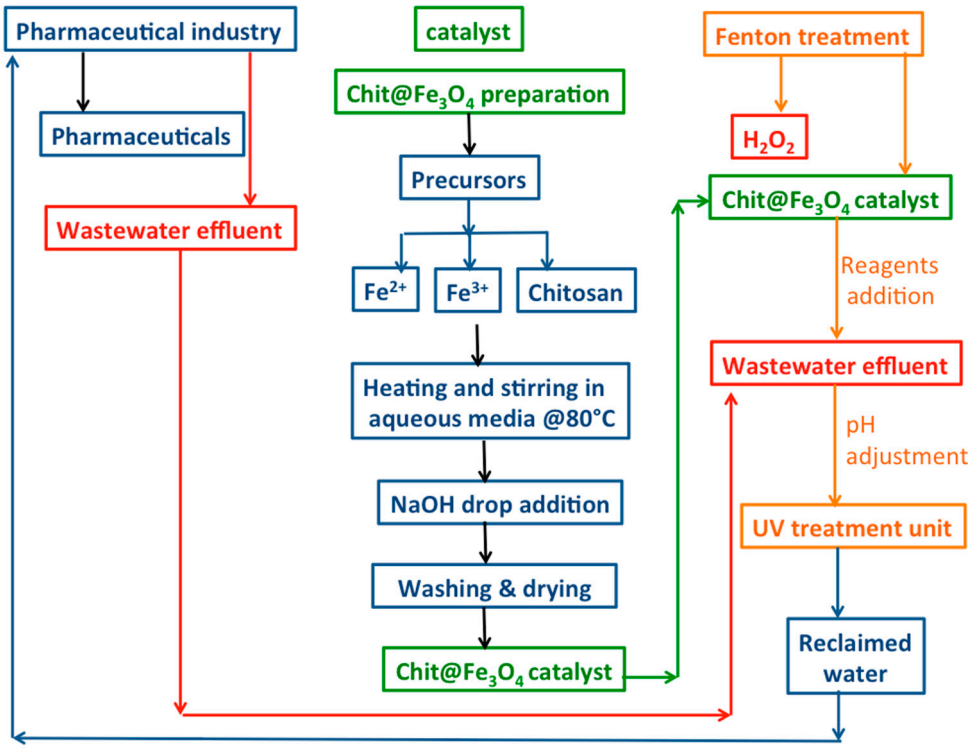

Figure 1. Graphical illustration of the experimental procedure.

2.3. Characterization of Chit@Fe_3O_4

The X-ray diffraction (XRD) pattern of the Chit@Fe_3O_4 nanoparticles was examined using a Bruker–Nonius Kappa CCD diffractometer (Baton Rouge, LA, USA) equipped with CuKα radiation (λ = 1.5406 Å). The XRD analysis covered a 2θ range of 10 to 80°.

To investigate the morphology of the Chit@Fe_3O_4 composite, a transmission electron microscope (TEM) (Tecnai G20), Beijing, China, FEI, and a field-emission scanning electron microscope (SEM) (Quanta FEG 250) were utilized. In the TEM analysis, typical magnification values of ×8000 and ×60,000 were employed. Additionally, SEM investigation was complemented by energy dispersive X-ray spectroscopy (EDX) for elemental composition analysis of the samples. The particle size distribution of the Chit@Fe_3O_4 composite was determined using the IMAGEJ 1.48 V program.

Furthermore, the Fourier transform infrared (FTIR) analysis was conducted in the wavenumber region of 400–4000 cm^{-1} using a Jasco FTIR-4100 spectrometer (Darmstadt, Germany). Also, the FTIR analysis was performed in the region of 400–4000 cm^{-1} using Jasco FTIR-4100 spectrometer. Also, diffuse reflectance spectroscopy (DRS) was used to investigate the optical characteristics of the photocatalyst.

3. Results and Discussion

3.1. Characterization of the Prepared Chit@Fe_3O_4 Composite

3.1.1. XRD Analysis of Chit@Fe_3O_4

The X-ray diffraction (XRD) pattern of the composite substance was investigated and compared with that of the pristine magnetite material. JCPDS card No. 19-0629 was used as a reference of the magnetite substance. Commonly, the standard pattern of magnetite peaks at 30.06°, 35.29°, 43.05°, 53.05°, 57.15°, and 62.61° correspond to the (220), (311), (400), (422), (511), and (440) planes, respectively, of Bragg's reflections for FCC structures. The data displayed in Figure 2 show the main phases of both the chitosan and magnetite nanoparticles in the composite material. The diffraction peaks at relative intensities of 2θ (18.30, 30.05, 35.49, 43.22, 53.63, 57.06, 62.48, and 74.24°) reflect the presence of magnetic nanoparticles. Such diffraction peaks correspond to the planes [(111), (220), (311), (400),

(422), (511), (440), (533)], respectively. Thus, according to the graph of the Fe_3O_4 phase, these planes and relative intensities confirm the presence of magnetite in the composite. Moreover, it is noteworthy to mention that sample is characterized as highly crystalline in nature, and the peak broadening demonstrates the small particle size of the material. The crystallite size was estimated to be 26.48 nm via the Scherrer equation using the width of the most extensive XRD peak. Also, the amorphous nature of chitosan is apparent in the sample and is revealed at the 2θ of 20. Notably, amorphous chitosan material was decorated with Fe_3O_4 nanoparticles without changes in the magnetite phase.

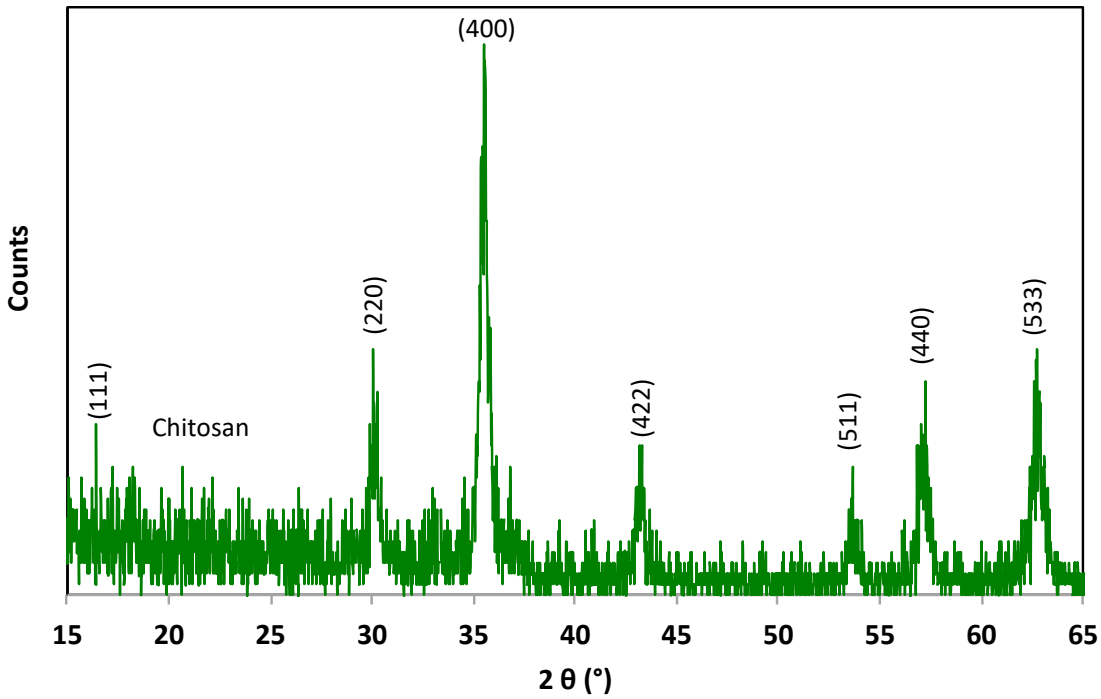

Figure 2. XRD pattern of the synthesized Chit@Fe_3O_4 nanoparticle composite substance.

3.1.2. TEM Analysis and Particle Size of Chit@Fe_3O_4

Transmission electron microscopy (TEM) was employed to investigate the morphology of the Chit@Fe_3O_4 composite. Also, the particle size distribution was investigated via digital TEM images and the IMAGEJ 1.48 V program. The images in Figure 3a display the TEM micrograph of the chitosan-augmented magnetite nanoparticles. The magnetite particles display a spherical shape with a predominant size of 12.5 nm (Figure 3b). The dark, dense spheres indicate the crystalline magnetite phase, whereas the bright areas correspond to amorphous chitosan. It is noteworthy that some particles are agglomerated together since the attraction forces between the magnetite particles consists of dipole forces. In addition, to confirm the presence of chitosan in the composite, a TEM image of pristine magnetite nanoparticles is presented in Figure 3c. This image displays dark, dense spherical particles without the presence of bright areas that reflects chitosan.

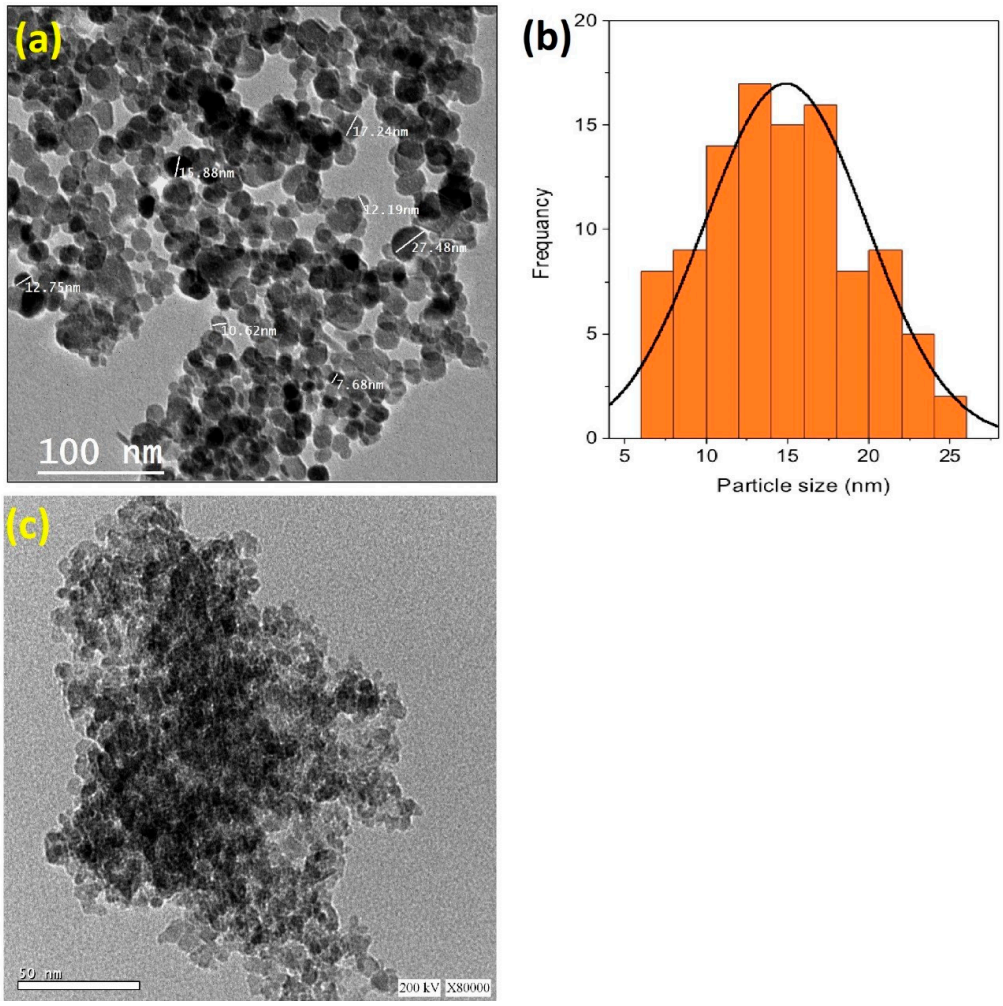

Figure 3. TEM micrograph (**a**) augmented with the particle size distribution histograms (**b**) of the synthesized Chit@Fe_3O_4 nanoparticles composite substance, and the TEM micrograph of pure magnetite nanoparticles (**c**).

3.1.3. SEM Morphology of Chit@Fe_3O_4

The morphology of the prepared Chit@Fe_3O_4 photocatalyst was assessed through SEM analysis, and the images are displayed in Figure 4a,b. The SEM pictures with different magnifications exhibit agglomerated nanoparticles. Chitosan crosslinker plays a significant role in investigating the better spherical morphology of nanoparticles. The spherical shape of the nanoparticles corresponds to the narrow grain size distribution of magnetite. Also, the chitosan was loaded with spherical particles of magnetite, as shown in the SEM image. For the purposes of comparison and verifying the presence of chitosan in the sample, an SEM image of the pure magnetite sample is presented in Figure 4c. These images illustrate the differences between the composite (Figure 4a) and pure magnetite (Figure 4c) in the presence of chitosan particles since the rough surface of the magnetite nanoparticles is more clearly visible in the pure magnetite image.

In addition, the elemental composition of the prepared sample was attained through energy dispersive X-ray spectroscopy (EDX) analysis; the shares of iron, oxygen, and carbon are 53.13, 32.86, and 45.14%, respectively (Figure 4d). The results obtained confirmed no other impurities have been detected in the prepared composite (Chit@Fe_3O_4), verifying the presence of a nanoparticle composite matrix comprising only iron, oxygen, and carbon.

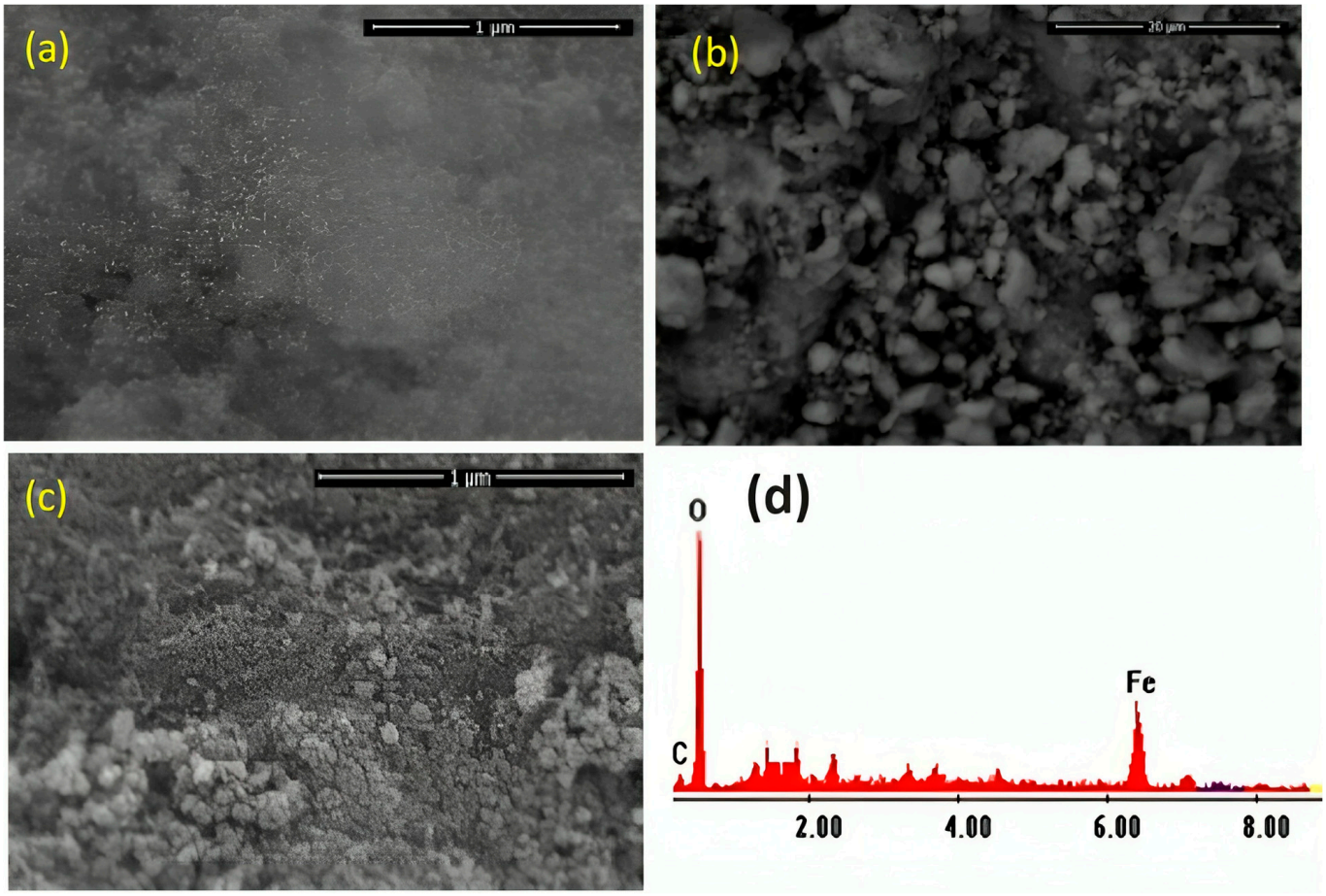

Figure 4. SEM images of the synthesized Chit@Fe_3O_4 nanoparticles composite substance at different imaginations (**a**,**b**), magnetite nanoparticles (**c**), and EDX analysis (**d**).

3.1.4. FTIR Analysis and Optical Characteristics

The FTIR spectra of the prepared sample Chit@Fe_3O_4 is evaluated to verify the encapsulation of Fe_3O_4 nanoparticles by chitosan and the formation of the composite. The spectral data shown in Figure 5a depict the range from 400 to 4000 cm^{-1}. The infrared (IR) spectrum of chitosan exhibited distinct absorption bands, such as a peak at 3429 cm^{-1}, which corresponds to the stretching vibrations of the –NH or –OH groups. Additionally, the peaks observed at 2919 cm^{-1} and 1469 cm^{-1} were attributed to the stretching vibrations of the –CH groups in the chitosan copolymer. The presence of chitosan was further confirmed by the appearance of the amide II bands at 1632 cm^{-1} (–NH bending) and 1469 cm^{-1} (CN stretching). Furthermore, the characteristic peak observed at 558 cm^{-1} indicates the stretching vibration of iron oxide nanoparticles, specifically the Fe–O stretching vibration. Another notable peak can be observed at 2919 cm^{-1}, which corresponds to the stretching vibration of –CH groups [25].

UV–Vis DRS studies were conducted on the Chit@Fe_3O_4 composite to examine the optical characteristics of the catalyst. The DRS of the sample is defined by a main band with a maximum band peak at around 260 nm (Figure 5b). This peak was assigned to a surface plasmon resonance typical of magnetite nanoparticles [7].

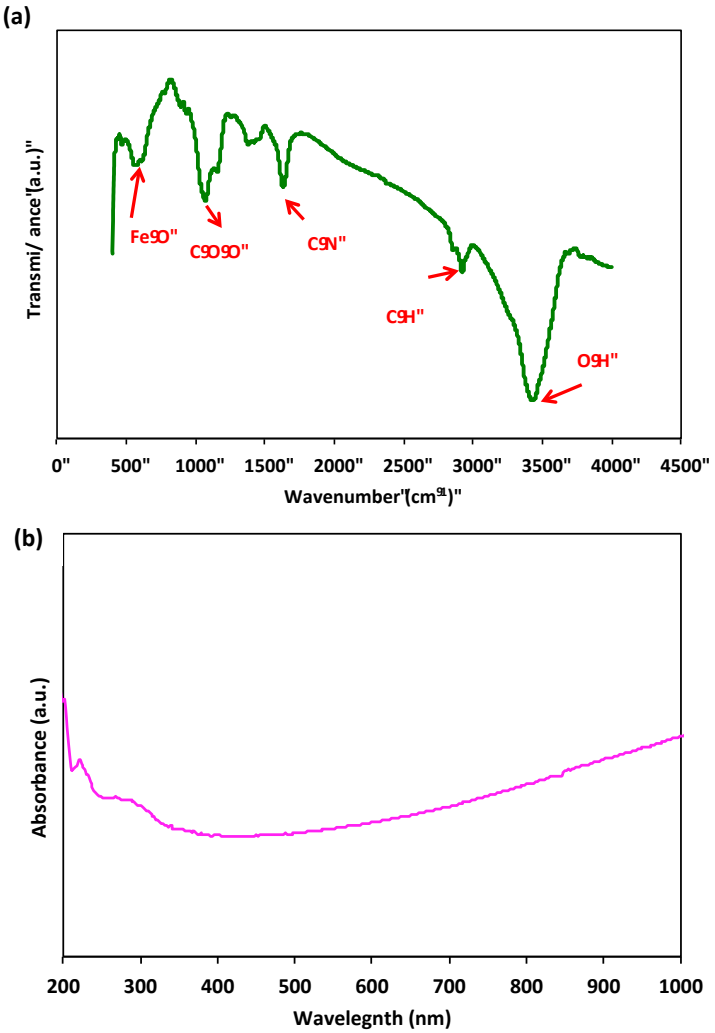

Figure 5. FTIR spectrum of Chit@Fe_3O_4 composite (**a**) and UV-Vis DRS absorption spectrum (**b**).

3.2. Application of Chit@Fe_3O_4 Composite in Acetaminophen Oxidation

3.2.1. Effect of Reaction Time in Different Systems

Figure 6 is jointly exhibits the reaction time of oxidation via various treatment systems. The catalytic oxidation of acetaminophen by the modified oxidation Fenton system based on the Chit@Fe_3O_4 nanocomposite is compared to that induced by the solo system of Chit@Fe_3O_4 as well as the pristine H_2O_2 systems under the ultraviolet irradiance. In addition, the augmented H_2O_2/Chit@Fe_3O_4 was further investigated regarding its role as a dark oxidation system for comparison with the photo-Fenton system and to clarify the role of this modified photo-Fenton reaction. Furthermore, to illustrate the role of the Fenton reaction, an adsorption test using such material (Chit@Fe_3O_4) was also conducted using the applied catalyst without hydrogen peroxide addition or ultraviolet radiation. The efficacy of such treatment was tested in the terms of acetaminophen removal.

The results displayed in Figure 6 illustrate that 52% of removal was associated with the H_2O_2/Chit@Fe_3O_4 subjected to ultraviolet irradiance. However, the removal value deduced to 35, 21, and 8% when the acetaminophen removal was attained through H_2O_2/UV, Dark Chit@Fe_3O_4, and Chit@Fe_3O_4/UV treatments, respectively. It is noteworthy that in all systems, the initial removal rate is significant and then steadily decreases. However, the removal rate reaches its peak of 52% when the Fenton system is applied under UV irradiance. This could be illustrated by $Fe^{2+/3+}$, which is exhibited in this composite and was augmented by hydrogen peroxide, resulting in a Fenton system that generates oxidizing hydroxyl radical species. However, the solo system catalyst and hydrogen peroxide can

only lead to limited hydroxyl radical generation [21]. Hence, the number of OH radicals produced via the Fenton-based Chit@Fe_3O_4 is higher, and this might provide a positive effective in acetaminophen treatment and the oxidation reaction. In addition, it is essential to mention that the nanoscale size particle size helps in improving oxidation since the available surface area is increased and hence the amount of OH generated is maximized. Thus, the overall reaction yield using nanosized particles is high. Furthermore, the use of the Chit@Fe_3O_4 as an adsorbent material under the same conditions results in a reduction of only 4%. These data indicate the capability of this material to be a photocatalyst, while it could also be an adsorbent material. In summary, the effect of material porosity in the adsorption test was greater than that in the oxidation reaction. This could be due to the mesoporous material exhibiting higher stability compared to the microporous substances. Pollutants have a tendency to become highly adsorbed within micropores, which can eventually lead to blockages and render them unavailable for subsequent use.

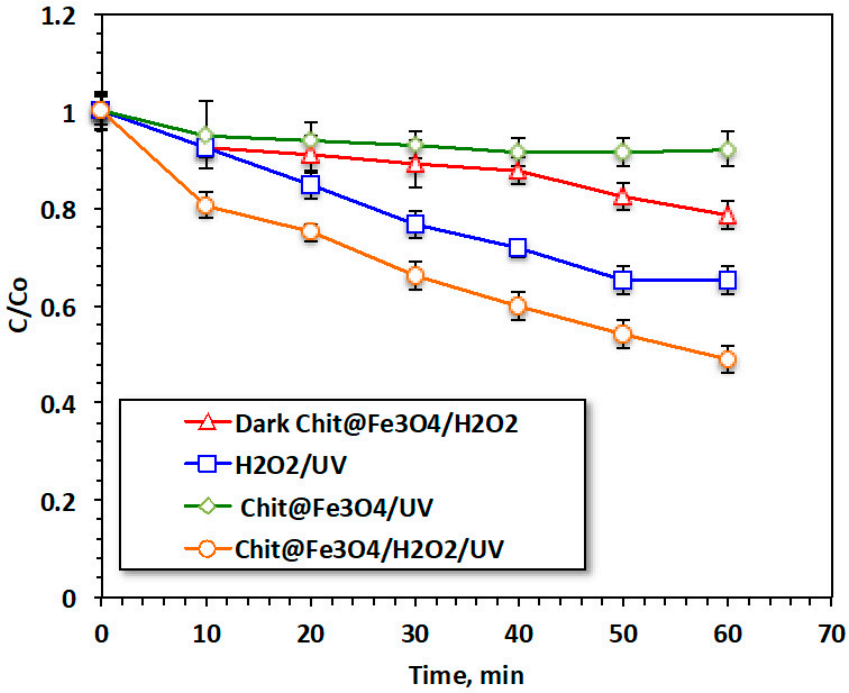

Figure 6. Reaction time effectiveness on different oxidative systems.

However, it is noteworthy that the pores size and diameter might have a minor effect on the oxidation reaction compared to the adsorption treatment. This minor effect on the oxidation reaction linked to the available pores in the catalyst is due to the faster diffusion of H_2O_2 within the pores of the material [26,27].

3.2.2. Effect of Acetaminophen Loading

To achieve practical applications, it is essential to investigate the acetaminophen concentration [9]; in this regard, initial acetaminophen concentration was varied, and the effect of pollutant loading on the oxidation performance was tested. The results shown in Figure 7 demonstrate the effectiveness of the modified Fenton oxidation (Chit@Fe_3O_4/UV) system with various acetaminophen loadings ranging from 10 to 100 mg/L, whereas all the other working variables were kept constant (20 and 200 mg/L for Chit@Fe_3O_4 and H_2O_2, respectively, and a pH of 2.0). The maximum removal efficacy with respect to acetaminophen from the aqueous solution reached 95% when the pollutant concentration was only 20 mg/L. However, when the acetaminophen increased (100 mg/L), the removal rate reduced to only 28%. This phenomenon was illustrated when the doses of Chit@Fe_3O_4 and H_2O_2 were kept constant in all experiments, whereas the acetaminophen increased.

Thus, the reduction and oxidation rate declined. It is noteworthy that the same trend of an initial rapid oxidation rate was observed for all pollutant loading; this is due to the high oxidation rate, which is linked to the abundant of hydroxyl radicals at the beginning of the reaction. However, with the progression of the reaction, the hydrogen peroxide was consumed, thereby reducing the number of OH radicals. The yield of •OH radicals was not sufficient to oxidize the pollutant in high concentration. Furthermore, the accessible active vacant adsorbent sites on the surface of Chit@Fe_3O_4 are not sufficient for adsorbing high load. Also, the Chit@Fe_3O_4 active sites being crowded with acetaminophen resulted in the effective number of •OH radicals being diminished. Similar results is previously reports in literature [27] for treating chloride using a Fenton oxidation system.

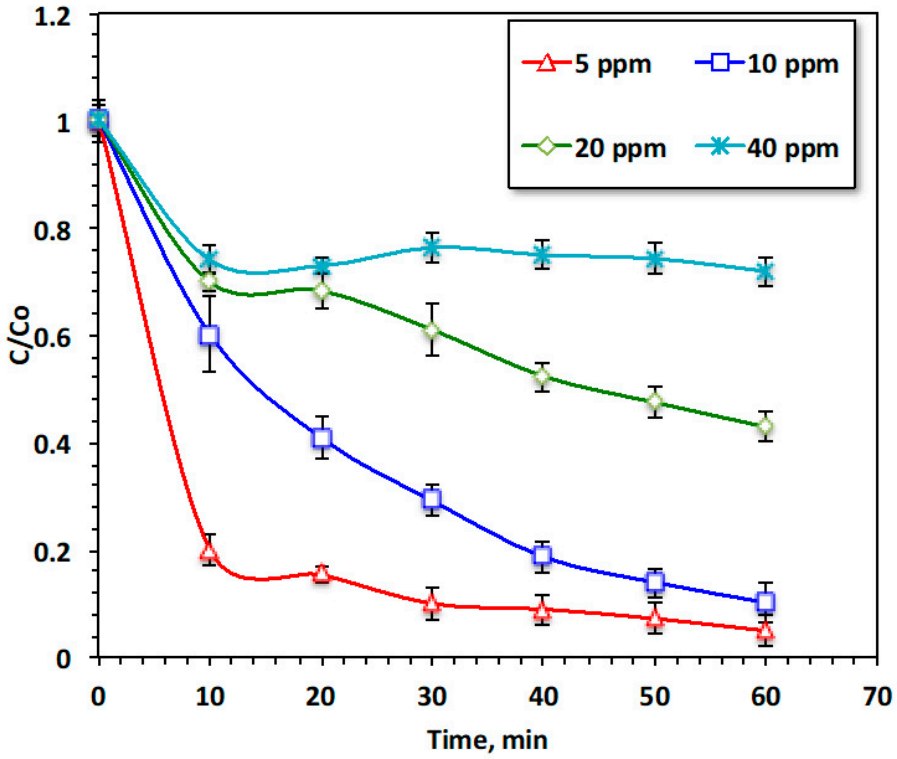

Figure 7. Effect of acetaminophen loading on the oxidation system.

3.2.3. Effect of Chit@Fe_3O_4 Concentration

The strong oxidative radical (˙OH) is the main responsible for oxidizing acetaminophen in the modified Fenton reaction; however, this radical's production is mostly dependent on different Fenton variables. ˙OH radicals should be maximized to attain a high oxidation capacity. Also, since ˙OH radicals are responsible for a high oxidation rate, and their presence is linked to the optimal dose of a reagent, the predominant radical in the optimal reagent is the ˙OH radical.

Transition metal alteration in the Fenton system has a significant role in the oxidation reaction. According to studies performed by various authors [14,19], the Fenton reaction's yield is mainly dependent on the catalyst dose. Consequently, to ensure the function of the chitosan polymer and magnetite nanoparticles in the Chit@Fe_3O_4 composite in our modified Fenton system, different concentrations of the catalyst source, Chit@Fe_3O_4, ranging from 5 to 40 mg/L, were examined, whereas all other system parameters were kept at constant values of a pH of 3.0, 200 mg/L of H_2O_2, and room temperature. According to the data displayed in Figure 8, ˙OH radical production is associated with the amount of Chit@Fe_3O_4 in the reaction medium. The reaction rate is enhanced with the increase in the content of the catalyst. Acetaminophen removal is enhanced from 60 to 75 and 95% as the Chit@Fe_3O_4 concentration increases from 5 to 10 and 20 mg/L, respectively. However, a

further increase in the Chit@Fe_3O_4 concentration to 40 mg/L results in a reduction in the reaction rate, providing a removal rate of only 44%. This might be linked to the OH radicals becoming trapped by the excess Chit@Fe_3O_4 catalyst ions [28]. Remarkably, an excess concentration of the Chit@Fe_3O_4 reagent results in adverse effects of increased magnetite and chitosan doses on the reaction medium as the excess catalyst, especially the iron species in the aqueous media, impacts the reactive species of ˙OH radicals' functioning. A similar trend was previously reported in the literature [29,30]. Furthermore, Wulandari and his co-workers [22] verified that the critical dose of chitosan-coated Fe_3O_4 nanoparticles might affect treatment efficiency.

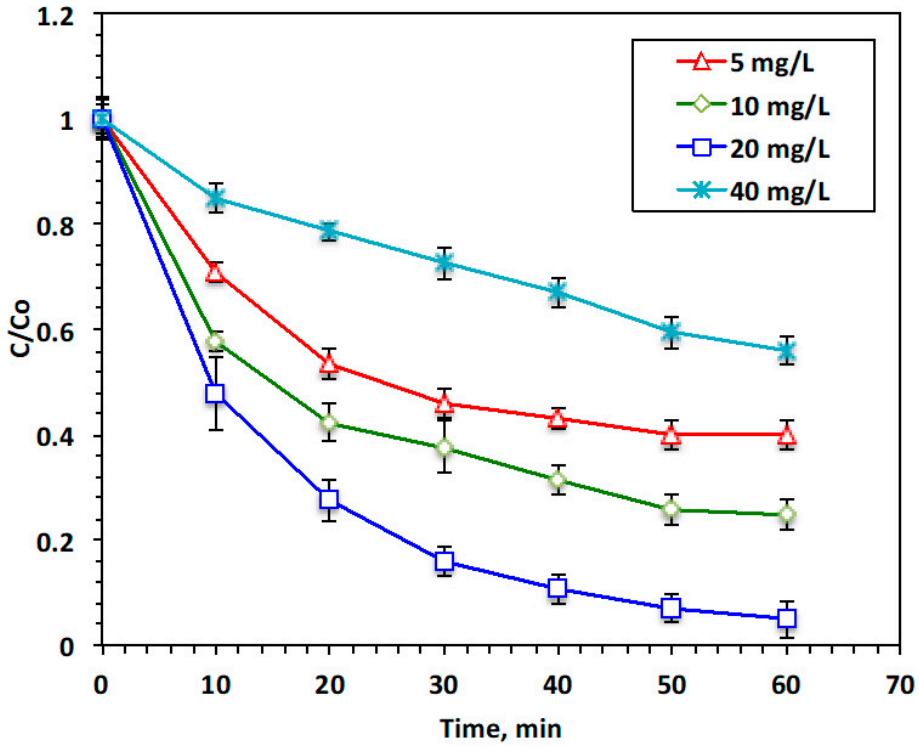

Figure 8. Effect of Chit@Fe_3O_4 catalyst loading on the Fenton oxidation system.

3.2.4. Effect of H_2O_2 Concentration

The hydrogen peroxide concentration in the Fenton system media has diverse effects on hydroxyl radical production and thus on the Fenton reaction's yield. Based on this concept, the hydrogen peroxide concentration in the reaction was set to be within the range from 50 to 400 mg/L to inspect the influence of this reagent on the current modified system (for 20 mg/L of Chit@Fe_3O_4 catalyst and a pH of 3.0), and the data of this experiment series are presented in Figure 9. The results reveal that acetaminophen oxidation increased from 40% to 84% with the elevation of the H_2O_2 dose from 50 to 200 mg/L, respectively. This increase can produce an extra yield of ˙OH radicals, which are the main responsible for the oxidation system. Hence, this increase in acetaminophen oxidation was predictable. However, further elevation indicates that this reagent can reduce the oxidation yield. This might be associated with a decline in the yield of ˙OH radicals since excess H_2O_2 results in the production of HO_2 radicals rather than OH radicals. These radicals reduce the oxidation rate rather than enhancing acetaminophen reduction. Also, the excess HO_2 radicals present in the reaction media react with the hydroxyl radicals and minimize their effect, thereby further lowering the overall reaction rate [31,32]. These findings were previously confirmed by Laib et al. (2021) [16] in treating reactive blue 19 using an oxidation reaction via a heterogeneous photo-Fenton catalyst.

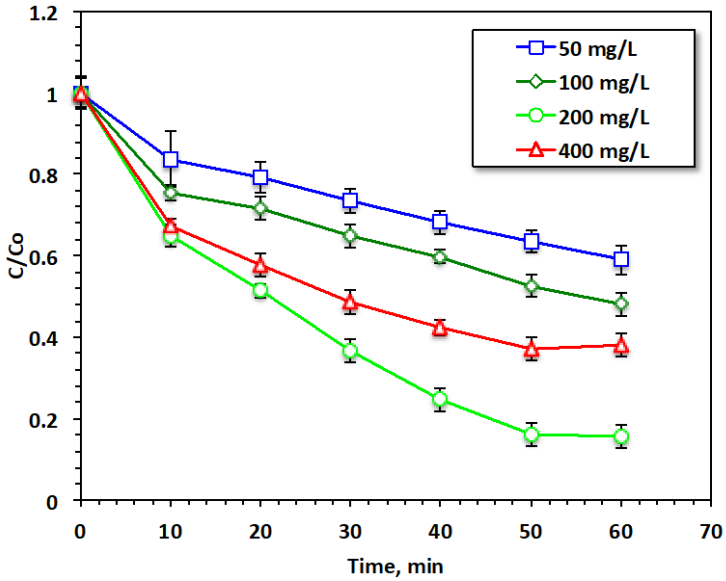

Figure 9. Effect of H_2O_2 loading on the Fenton oxidation system.

3.2.5. Effect of pH

The initial aqueous medium pH plays a significant role in the Fenton oxidation reaction. Conventionally, Fenton reaction is conducted at a highly acidic pH system, but this might change according to the reaction and catalyst type. In this regard, to examine the optimal operational pH value, the initial pH of the aqueous acetaminophen wastewater was assessed by changing the wastewater pH from 2.0 to 6.0. An investigation of the data displayed in Figure 10 demonstrated that the acidic range is preferable. Decreasing the pH to 2.0 revealed the optimal oxidation pH, corresponding to 95% compared to 89% at a pH of 6.0. This means although thane acidic pH is favorable, the current modified system could work at various pH values. It is noteworthy that $H_3O_2^+$ may be formed at an acidic pH, which might lead to an increase in peroxide stability. However, FeOOH is precipitated with an increase in the pH value, thus affecting the production yield of OH radicals [32,33].

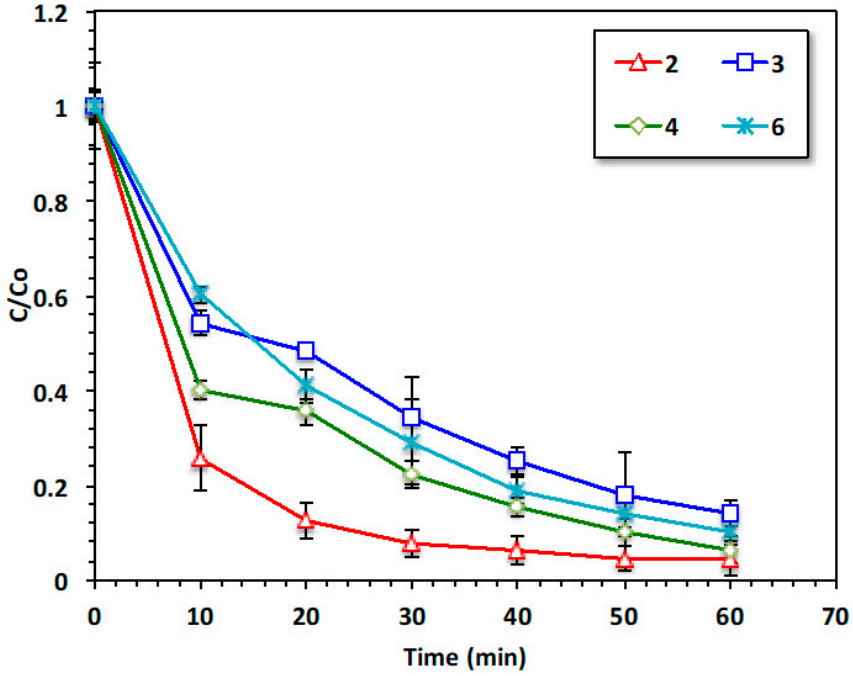

Figure 10. Effect of pH on the Fenton oxidation system.

3.2.6. Effect of Temperature

From the industrial and practical perspectives, it is crucial to establish the effect of temperature, since in real-scale applications, the discharge is attained at various temperatures. To establish the optimal working temperature, the temperature of the aqueous solution containing acetaminophen was altered with the temperature range from 26 to 60 °C, and the results of these experiments are exhibited in Figure 11. The rise in temperature indicated a significant deterioration in acetaminophen oxidation, with a subsequent reduction in the reaction yield. Room temperature provided the highest reaction oxidation yield, corresponding to the highest acetaminophen reduction, reaching 95%. This may be attributed to the high temperatures exceeding than room temperature resulting in a reduction in the oxidation efficiency due to the rapid reduction of H_2O_2 to O_2 and H_2O [34].

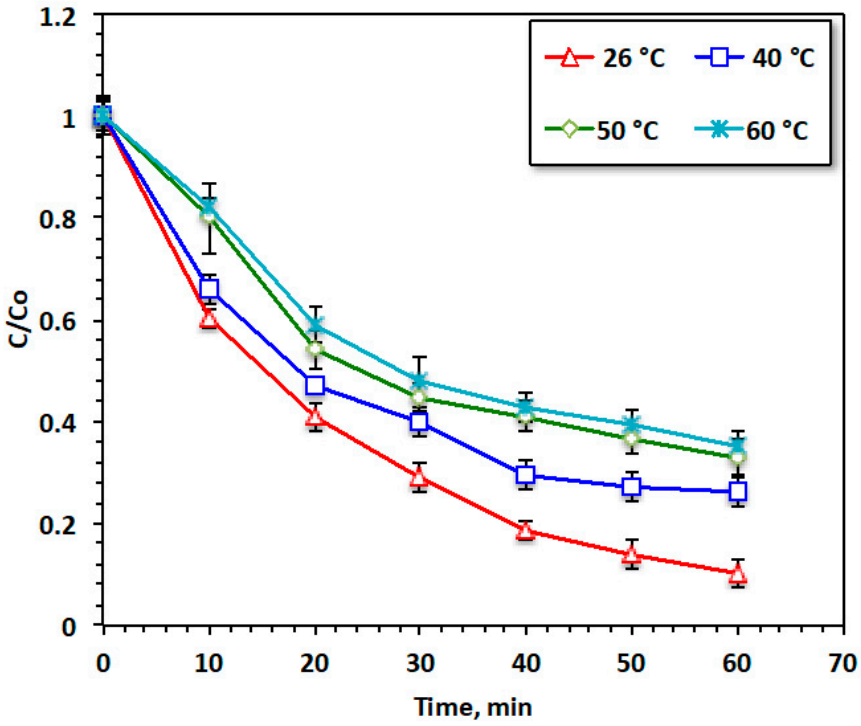

Figure 11. Effect of temperature on the Fenton oxidation system.

3.2.7. Kinetics and Thermodynamic Profile

The objective of investigating the effects of temperature on the oxidation system is twofold: to establish the overall kinetics and to consider the Arrhenius-type dependency of the global kinetic constant on temperature. This exploration is vital for large-scale treatment facilities [35], as it provides crucial information for reactor design and process economics.

Upon analyzing the data presented in Figure 10, it was observed that an increase in temperature had a negative impact on acetaminophen removal. The relationship between different operating temperatures and the reaction rates of zero-order, first-order, and pseudo-second-order kinetics is illustrated in Figure 12a–c, respectively. Table 1 presents the kinetic constants and parameters of the zero-order, first-order, and second-order kinetic models. The model with the highest R^2 value is considered the best fit, as a regression coefficient (R^2) close to 1 indicates a good fit to the proposed kinetic model.

Notably, the correlation coefficient R^2 values mentioned in previous studies [36,37] range from 0.933 to 0.9157 and from 0.9872 to 0.9962, further supporting the suitability of the kinetic models chosen for this study. Based on these findings, it can be inferred that the drug was transported from the studied systems through various mechanisms.

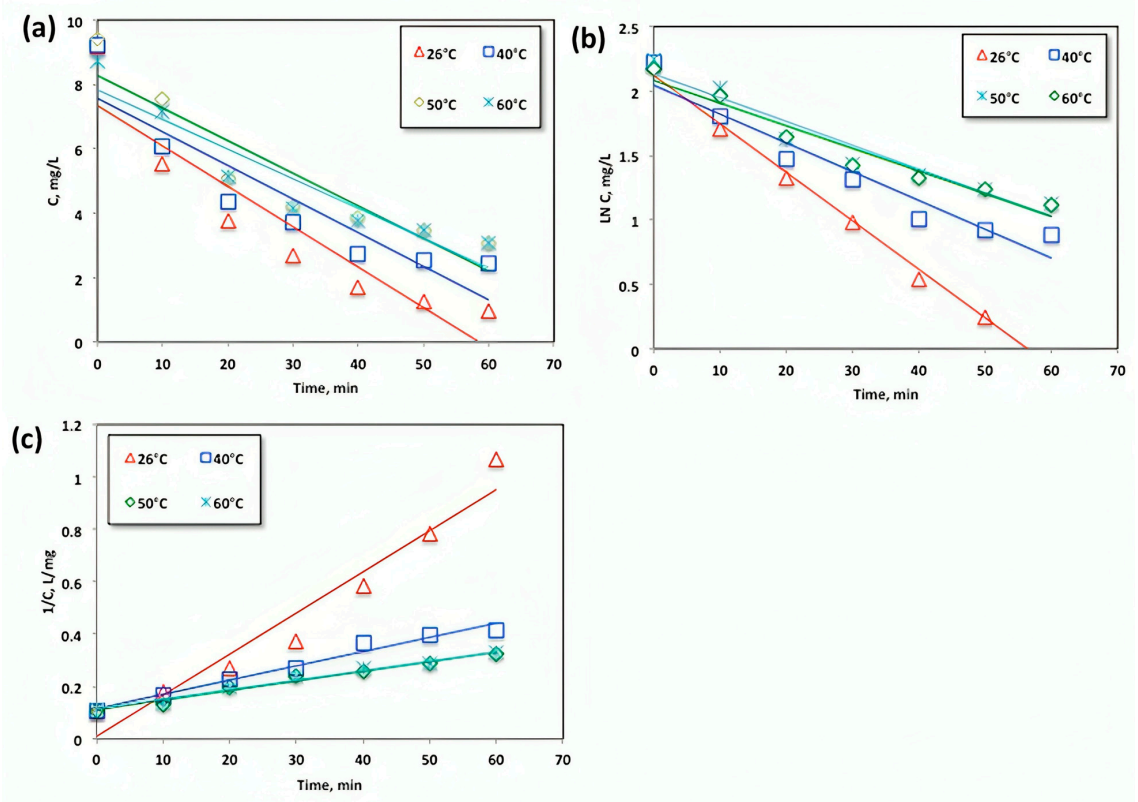

Figure 12. Plots of the (**a**) zero-, (**b**) first-, and (**c**) second-order kinetic models for the oxidation of acetaminophen with modified Fenton reagent at different temperatures.

Table 1. Kinetic parameters for different reaction order models for acetaminophen treatment in aqueous media *.

Kinetic Model	Parameters	T			
		299	**313**	**323**	**333**
Zero-order $C_t = C_o - k_o t$	k_o (min^{-1})	0.125	0.104	0.102	0.092
	$t_{1/2}$	36.60	44.35	46.13	47.39
	R^2	0.85	0.82	0.85	0.88
First-order $C_t = C_o - e^{k_1 t}$	k_1 (min^{-1})	0.038	0.022	0.018	0.017
	$t_{1/2}$	40.76	38.5	31.5	18.241
	R^2	0.99	0.93	0.93	0.94
Second-order $\left(\frac{1}{C_t}\right) = \left(\frac{1}{C_0}\right) - k_2 t$	k_2 (L/gm.min)	0.0157	0.0054	0.004	0.0036
	$t_{1/2}$	6.96	20.07	26.56	31.85
	R^2	0.95	0.97	0.98	0.99

* C_o and C_t: initial and at time t acetaminophen concentration (mg/L)); t: time (min); k_0, k_1, and k_2: kinetic rate constants of zero-, first-, and second-orders kinetic models.

Based on the data presented in Figure 12 and Table 1, it is evident that the regression coefficients (R^2) attained from Figure 12 and displayed in Table 1 are the highest for the second-order reaction model, which effectively represents the experimental data. The second-order reaction rate constants range from 0.0157 to 0.0036 L/mg.min as the temperature increases. Additionally, the half-life time ($t_{1/2}$) increases with higher temperatures. The shortest ($t_{1/2}$) for acetaminophen oxidation was calculated at a temperature of 26 °C. Therefore, the second-order model accurately predicts the oxidation yield within the tem-

perature range up to 26 °C. Previous studies [35] have also reported that the Fenton reaction is governed by second-order kinetics, supporting these findings.

Thermodynamic variables were verified to further support the oxidation of the modified Fenton system, and the data are tabulated in Table 2. Based on the second-order kinetic rate constant, the Arrhenius principle $\left(k_2 = Ae^{\frac{-Ea}{RT}}\right)$ could be written in the linearized form $\left(\ln k_2 = \ln A - \frac{Ea}{RT}\right)$, where A and R are constants of the pre-exponential factor and gas constant; T is the temperature; and Ea is the activation energy attained from the linear correlation of $\ln k_2$ and $-1/T$, corresponding to 36.35 kJ/mol. Hence, this result of minimal energy confirms that the acetaminophen oxidation proceeds at a low energy barrier. Various authors [36,37] have recorded similar results in treating textile dying wastewater and petroleum refinery effluents, respectively, using a Fenton system. Furthermore, Eyring's relation, $k_2 = \frac{k_B T}{h} e^{\left(-\frac{\Delta G'}{RT}\right)}$ [37], was applied to estimate the Gibbs free energy of activation ($\Delta G'$), where k_B and h are constants of Boltzmann and Planck', respectively. Also, both the enthalpy ($\Delta H'$) and entropy ($\Delta S'$) of activation were explored according to the following relations:

$$\Delta H' = E_a - RT \text{ and } \Delta S' = \left(\Delta H' - \Delta G'\right)/T,$$

respectively [38], and the data displayed in Table 2. According to the data demonstrated in Table 2, the positive values of $\Delta G'$ that increased with the temperature indicate the non-spontaneous nature of the reaction. Also, the positive values of $\Delta H'$ indicate the exothermic nature of the reaction. $\Delta S'$ is negative which confirms the non-spontaneity of the reaction. These results indicate that a decline in the degrees of freedom of the acetaminophen molecules, in addition to a high production yield of the OH radicals, thus increasing the oxidation rate. Pervious results in the literature are in accordance with these data [38].

Table 2. Thermodynamic data of acetaminophen oxidation via Chit@Fe_3O_4 based Fenton system.

	T/°C			
	26 °C	**40 °C**	**50 °C**	**60 °C**
Ea (kJ/mol)		36.35		
ΔG′ (kJ/mol)	83.56	90.37	94.15	97.43
ΔH′ (kJ/mol)	33.87	33.75	33.67	33.59
ΔS′ (kJ/mol.K)	−166.18	−180.88	−187.23	−191.74

3.2.8. Catalyst Stability and Reusability

Since chitosan augmented magnetite nanoparticles are a heterogeneous catalyst source, their recovery from aqueous media is possible [8]. It is essential to verify a catalyst's stability to ensure the sustainability of a given approach. In this regard, the cyclic use of Chit@Fe_3O_4 was conducted. After use, the catalyst is collected and then subjected for successive uses and then washed with distilled water in three washing cycles prior to being dried (1 h at 105 °C). Afterwards, the retrieved material was then used for acetaminophen oxidation at the optimal reagent doses of 20 and 200 mg/L of Chit@Fe_3O_4 and H_2O_2, respectively, and a pH of 2.0. The results displayed in Figure 13 explore the successive use of Chit@Fe_3O_4, demonstrating a reduction in catalyst activity. Catalyst reactivity was reduced, achieving an acetaminophen removal of only 69% in the fourth cycle compared to 95% for the fresh catalyst use, as seen in Figure 13. However, it is notable that even though the activity of the catalyst was reduced, it could still oxidize the acetaminophen material. Thus, these results verify the catalyst sustainability. Also, they confirm the catalyst's stability since chitosan-augmented magnetite nanocomposites exploits physicochemical stability [41].

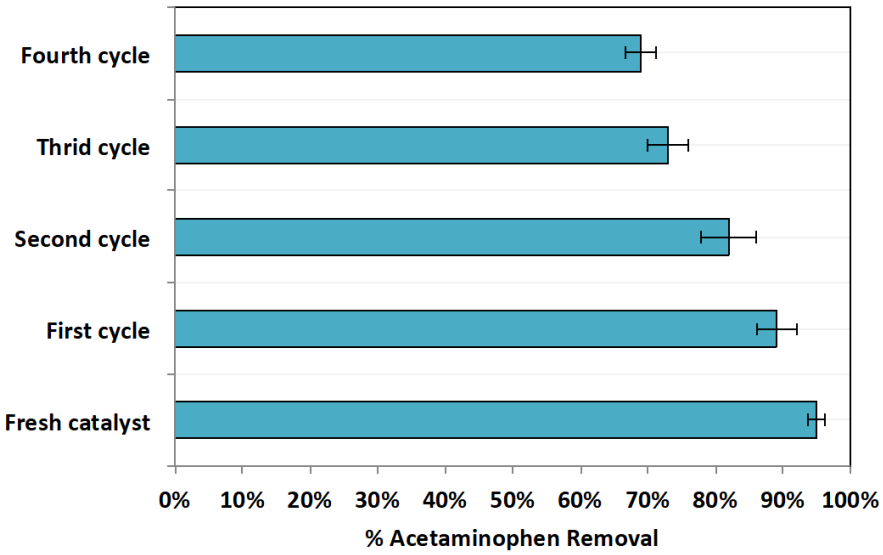

Figure 13. Chit@Fe_3O_4 cyclic use competence.

3.2.9. Oxidation Mechanism

The Fenton reaction system based on Chit@Fe_3O_4 basically comprises Fe^{2+} and Fe^{3+}, as well as chitosan. Conventionally, a catalyst is oxidized via the reagent H_2O_2 to generate the •OH species (Equation (1)), which are the main species responsible for oxidation, initiating the reaction between ions of iron and the hydrogen peroxide reagent. In this concept, the produced radicals attack the aromatic ring in the acetaminophen material and oxidize it into non-harmful end products, namely, CO_2 and H_2O. The presence of iron in this reaction acts as the rate-limiting step. Also, further radicals are generated, i.e., OH^- and $OH_2^{\bullet}$, as well as oxygen radicals that promote the cyclic reaction. However, H_2O_2 can decay due to the presence of dissolved oxygen. The radicals' mechanism is illustrated in Equations (1)–(8). Additionally, the hydrolyzed iron ions in the reaction media help in the formation of further radicals due to the reaction with hydrogen peroxide (Equations (9) and (11)). Moreover, UV illumination results in the generation of additional ·OH radicals (Equations (13)–(15)).

$$Fe^{2+} + H_2O_2 \rightarrow Fe^{3+} + OH^- + OH^{\bullet} \quad (1)$$

$$Fe^{3+} + OH_2^{\bullet} \rightarrow Fe^{2+} + O_2 + H^+ \quad (2)$$

$$H_2O_2 + HO^{\bullet} \rightarrow H^{\mp} + O_2^{\bullet} + H_2O \quad (3)$$

$$Fe^{3+} + H_2O_2 \rightarrow Fe^{2+} + OH_2^{\bullet} + H^+ \quad (4)$$

$$H_2O_2 + HO^{\bullet} \rightarrow HO_2^{\bullet} + H_2O \quad (5)$$

$$Fe^{2+} + OH^{\bullet} \rightarrow Fe^{3+} + OH^- \quad (6)$$

$$OH^{\bullet} + OH^{\bullet} \rightarrow H_2O_2 \quad (7)$$

$$2OH_2^{\bullet} \rightarrow H_2O_2 + O_2 \quad (8)$$

$$Fe^{2+} + OH_2^{\bullet} + H^+ \rightarrow Fe^{3+} + H_2O_2 \quad (9)$$

$$OH^{\bullet} + Fe^{2+} \rightarrow Fe^{3+} + OH^- \quad (10)$$

$$H_2O_2 + HO_2^{\bullet} \rightarrow H_2O + O_2 + HO^{\bullet} \quad (11)$$

$$Fe^{2+} + H_2O_2 + hv \rightarrow Fe^{3+} + OH^- + OH^{\bullet} \quad (12)$$

$$Fe(OH)^{2+} + hv \rightarrow Fe^{2+} + H^+ \quad (13)$$

$$H_2O_2 + hv \rightarrow 2OH^{\bullet} \quad (14)$$

$$HOO^{\bullet} + H_2O_2 \rightarrow H_2O + O_2 + HO^{\bullet} \quad (15)$$

Subsequently, due to the presence of hydroxyl radicals in the reaction medium, hydrogen is abstracted, and this provides a macro radical beside the chitosan, which results in the growth of attached monomers. In addition, chitosan produce excess OH radicals due to its chelating characteristics with respect to metals (Equations (16) and (17)) [42–46]. Thus, overall, the generated radicals attack the aromatic ring of the acetaminophen and oxidize it (Equation (18)).

$$OH^{\bullet} + polysscharide - H \rightarrow H_2O + Polysaccharide^{\bullet} \quad (16)$$

$$Polysaccharide^{\bullet} + Monomer \rightarrow OH^{\bullet} + polysscharide - g - polymer \quad (17)$$

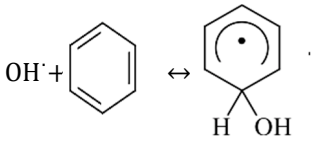

$$\rightarrow \text{Further reactions} \quad (18)$$

Furthermore, to evaluate the significant species that control the oxidation in the modified photo-Fenton system, various scavengers were tested and added to the reaction medium (Figure 14). These scavengers were added independently and separately to trap and remove specific active species. Initially, ammonium oxalate was added to the reaction medium to reflect the deterioration of the holes (h^+) present in the catalyst. This addition results in a scavenging effect in the reaction, and the oxidation efficiency declined from 95% to 58%. Also, the addition of isopropanol was examined to investigate the scavenging effect of the superoxide radical ($\bullet O_2^-$). The results of this test revealed that the reaction oxidation efficiency of acetaminophen is also decreased to be 91%, which means that the terminal effect of the superoxide radical affects the oxidation efficiency. Finally, the effect of hydroxyl radical species on acetaminophen oxidation was investigated through the use of the benzoquinone scavenger in the reaction medium. The results of this experiment, leading to a massive scavenging effect, displayed only 15% oxidation. Such a dramatic reduction in oxidation efficiency reflects the importance of the hydroxyl radicals (OH) in the photo-oxidation activity. Hence, the presence of holes in the composite material affects the reaction, but the major effect is linked to the hydroxyl radical. However, a minor effect is related to the superoxide radical.

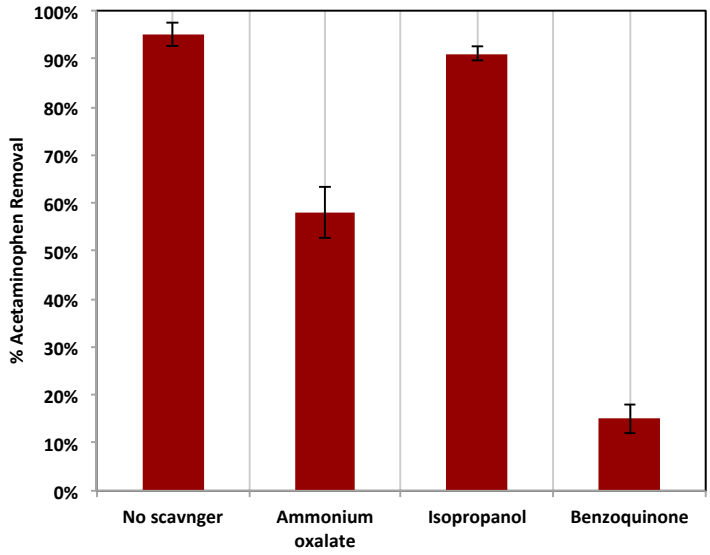

Figure 14. Effects of various scavengers on the photocatalytic oxidation of acetaminophen using Chit@Fe_3O_4 based Fenton system.

4. Conclusions

Chitosan coated with magnetite nanoparticles, constituting an environmentally sustainable catalyst, prepared through a co-precipitation route, and then augmented with H_2O_2, is a promising photocatalyst. This type of Fenton system was applied to oxidize acetaminophen, an emerging pollutant, in aqueous effluents. The oxidation reaction revealed that catalyst and H_2O_2 concentrations limit the oxidation process. Although an acidic pH is favorable, the oxidation process can proceed at a wide range of pH values. The experimental results showed that the oxidation time was achieved after one hour of illumination. Also, concentrations of Chit@Fe_3O_4 and H_2O_2 of 20 and 200 mg/L, respectively, are essential to complete the oxidation reaction of acetaminophen at a pH of 2.0 to achieve 95% removal. The sustainability of the catalyst was verified, and a 69% removal rate was reached in the fourth cyclic use. Furthermore, elevating the temperature is unfavorable, and an ambient temperature is efficient in providing a high acetaminophen oxidation rate. The kinetic modeling exhibiting that oxidation follows the second-order kinetic rate, with a minimum value of activation energy. Thus, the suggested catalyst is a viable option for treating pharmaceutical effluents in an environmentally benign way. However, further research is still required to assess its real-world applications on a larger scale. Moreover, to reach the scale of industrial practical applications, our results could be scaled up for industrial wastewater treatment plants. Also, appropriate catalyst doses could be statistically optimized for design and applications. More data are essential for solar applications plants to satisfy the industrial sector. Finally, it is noteworthy that the suggested system is a promising technology for the green treatment of emerging pollutants.

Author Contributions: Conceptualization, M.M.N. and M.A.T.; Methodology, M.M.N. and M.A.T.; Writing—original draft, M.M.N. and M.A.T.; Writing—review & editing, M.M.N. and M.A.T. All authors have read and agreed to the published version of the manuscript.

Funding: The authors extend their appreciation to Prince Sattam bin Abdulaziz University for funding this study through project number (PSAU/2023/01/27377).

Data Availability Statement: Data are available upon request.

Conflicts of Interest: The authors declare no conflict of interest.

References

1. Abdou, K.A.; Mohammed, A.N.; Moselhy, W.; Farghali, A.A. Assessment of modified rice husk and sawdust as bio-adsorbent for heavy metals removal using nano particles in fish farm. *Asian J. Anim. Vet. Adv.* **2018**, *13*, 180–188. [CrossRef]
2. Adesina, O.A.; Abdulkareem, F.; Yusuff, A.S.; Lala, M.; Okewale, A. Response surface methodology approach to optimization of process parameter for coagulation process of surface water using Moringa oleifera seed. *S. Afr. J. Chem. Eng.* **2019**, *28*, 46–51. [CrossRef]
3. Ahmadi, M.; Behin, J.; Mahnam, A.R. Kinetics and thermodynamics of peroxydisulfate oxidation of Reactive Yellow 84. *J. Saudi Chem. Soc.* **2016**, *20*, 644–650. [CrossRef]
4. Al, M.F.; Mo'ayyad, S.; Ahmad, S.; Mohammad, A.-S. Impact of Fenton and ozone on oxidation of wastewater containing nitroaromatic compounds. *J. Environ. Sci.* **2008**, *20*, 675–682.
5. Argun, M.E.; Karatas, M. Application of Fenton process for decolorization of reactive black 5 from synthetic wastewater: Kinetics and thermodynamics. *Environ. Prog. Sustain. Energy* **2011**, *30*, 540–548. [CrossRef]
6. Bounab, L.; Iglesias, O.; González-Romero, E.; Pazos, M.; Sanromán, M.Á. Effective heterogeneous electro-Fenton process of m-cresol with iron loaded actived carbon. *RSC Adv.* **2015**, *5*, 31049–31056. [CrossRef]
7. Clark, J.H.; Farmer, T.J.; Herrero-Davila, L.; Sherwood, J. Circular economy design considerations for research and process development in the chemical sciences. *Green. Chem.* **2016**, *18*, 3914–3934. [CrossRef]
8. Di, L.; Yang, H.; Xian, T.; Liu, X.; Chen, X. Photocatalytic and photo-Fenton catalytic degradation activities of Z-scheme Ag2S/BiFeO3 heterojunction composites under visible-light irradiation. *Nanomaterials* **2019**, *9*, 399. [CrossRef]
9. El-Desoky, H.S.; Ghoneim, M.M.; El-Sheikh, R.; Zidan, N.M. Oxidation of Levafix CA reactive azo-dyes in industrial wastewater of textile dyeing by electro-generated Fenton's reagent. *J. Hazard. Mater.* **2010**, *175*, 858–865. [CrossRef]
10. Golka, K.; Kopps, S.; Myslak, Z.W. Carcinogenicity of azo colorants: Influence of solubility and bioavailability. *Toxicol. Lett.* **2004**, *151*, 203–210. [CrossRef] [PubMed]
11. Guan, S.; Yang, H.; Sun, X.; Xian, T. Preparation and promising application of novel $LaFeO_3$/BiOBr heterojunction photocatalysts for photocatalytic and photo-Fenton removal of dyes. *Opt. Mater.* **2020**, *100*, 109644. [CrossRef]

12. Guan, X.-H.; Chen, G.-H.; Shang, C. Re-use of water treatment works sludge to enhance particulate pollutant removal from sewage. *Water Res.* **2005**, *39*, 3433–3440. [CrossRef]
13. Guedes, A.M.F.M.; Madeira, L.M.P.; Boaventura, R.A.R.; Costa, C.A.V. Fenton oxidation of cork cooking wastewater—Overall kinetic analysis. *Water Res.* **2003**, *37*, 3061–3069. [CrossRef]
14. Hilder, M.; Winther-Jensen, O.; Winther-Jensen, B.; MacFarlane, D.R. Graphene/zinc nano-composites by electrochemical co-deposition. *Phys. Chem. Chem. Phys.* **2012**, *14*, 14034–14040. [CrossRef] [PubMed]
15. Ioannou, L.A.; Fatta-Kassinos, D. Solar photo-Fenton oxidation against the bioresistant fractions of winery wastewater. *J. Environ. Chem. Eng.* **2013**, *1*, 703–712. [CrossRef]
16. Laib, S.; Rezzaz-Yazid, H.; Yatmaz, H.C.; Sadaoui, Z. Low cost effective heterogeneous photo-Fenton catalyst from drinking water treatment residuals for reactive blue 19 degradation: Preparation and characterization. *Water Environ. Res.* **2021**, *93*, 1097–1106. [CrossRef] [PubMed]
17. Li, X.; Cui, J.; Pei, Y. Granulation of drinking water treatment residuals as applicable media for phosphorus removal. *J. Environ. Manag.* **2018**, *213*, 36–46. [CrossRef] [PubMed]
18. Shangguan, Z.; Yuan, X.; Jiang, L.; Zhao, Y.; Qin, L.; Zhou, X.; Wu, Y.; Chew, J.W.; Wang, H. Zeolite-based Fenton-like catalysis for pollutant removal and reclamation from wastewater. *Chin. Chem. Lett.* **2022**, *33*, 4719–4731. [CrossRef]
19. Yuan, D.; Zhang, C.; Tang, S.; Li, X.; Tang, J.; Rao, Y.; Wang, Z.; Zhang, O. Enhancing CaO_2 fenton-like process by Fe(II)-oxalic acid complexation for organic wastewater treatment. *Water Res.* **2019**, *163*, 114861. [CrossRef]
20. Wang, L.; Wang, W.; Liu, M.; Ge, H.; Zha, W.; Wei, Y.; Fei, E.; Zhang, Z.; Long, J.; Sa, R. Understanding structure-function relationships in HZSM-5 zeolite catalysts for photocatalytic oxidation of isopropyl alcohol. *J. Catal.* **2019**, *377*, 322–331. [CrossRef]
21. Sun, X.; Huang, L.; Wang, G.; Feng, H.; Zhou, S.; Zhao, R.; Li, Z. Efficient degradation of tetracycline under the conditions of high-salt and coexisting substances by magnetic $CuFe_2O_4$/g-C_3N_4 photo-Fenton process. *Chemosphere* **2022**, *308*, 136204. [CrossRef] [PubMed]
22. Wulandari, I.O.; Mardila, V.T.; Santjojo, D.J.D.H.; Sabarudin, A. Preparation and characterization of chitosan-coated Fe_3O_4 nanoparticles using ex-situ co-precipitation method and tripolyphosphate/sulphate as dual crosslinkers. *IOP Conf. Ser. Mater. Sci. Eng.* **2018**, *299*, 012064. [CrossRef]
23. Xu, Z.; Fang, D.; Shi, W.; Xu, J.; Lu, A.; Wang, K.; Zhou, L. Enhancement in photo-fenton-like degradation of azo dye methyl orange using TiO_2/hydroniumjarosite composite catalyst. *Environ. Eng. Sci.* **2015**, *32*, 497–504. [CrossRef]
24. Yang, Y.; Ma, C.; He, X.; Li, J.; Li, M.; Wang, J. Calcined Aluminum Sludge as a Heterogeneous Fenton-Like Catalyst for Methylene Blue Degradation by Three-Dimensional Electrochemical System. *Electrocatalysis* **2021**, *12*, 698–714. [CrossRef]
25. Yin, Z.; Li, Y.; Song, T.; Bao, M.; Li, Y.; Lu, J.; Li, Y. Preparation of superhydrophobic magnetic sawdust for effective oil/water separation. *J. Clean. Prod.* **2020**, *253*, 120058. [CrossRef]
26. Duarte, F.; Maldonado-Hódar, F.J.; Pérez-Cadenas, A.F.; Madeira, L.M. Fenton-like degradation of azo-dye Orange II catalyzed by transition metals on carbon aerogels. *Appl. Catal. B Environ.* **2009**, *85*, 139–147. [CrossRef]
27. Amelia, S.; Sediawan, W.B.; Prasetyo, I.; Munoz, M.; Ariyanto, T. Role of the pore structure of Fe/C catalysts on heterogeneous Fenton oxidation. *J. Environ. Chem. Eng.* **2020**, *8*, 102921. [CrossRef]
28. Najjar, W.; Chirchi, L.; Santos, E.; Ghorhel, A. Kinetic study of 2-nitrophenol photodegradation on Al-pillared montmorillonite doped with copper. *J. Environ. Monit.* **2001**, *3*, 697–701. [CrossRef]
29. Oyewo, O.A.; Adeniyi, A.; Sithole, B.B.; Onyango, M.S. Sawdust-based cellulose nanocrystals incorporated with ZnO nanoparticles as efficient adsorption media in the removal of methylene blue dye. *ACS Omega* **2020**, *5*, 18798–18807. [CrossRef]
30. Pourali, P.; Behzad, M.; Arfaeinia, H.; Ahmadfazeli, A.; Afshin, S.; Poureshgh, Y.; Rashtbari, Y. Removal of acid blue 113 from aqueous solutions using low-cost adsorbent: Adsorption isotherms, thermodynamics, kinetics and regeneration studies. *Sep. Sci. Technol.* **2021**, *56*, 3079–3091. [CrossRef]
31. Rezgui, S.; Díez, A.M.; Monser, L.; Adhoum, N.; Pazos, M.; Sanromán, M.A. $ZnFe_2O_4$-chitosan magnetic beads for the removal of chlordimeform by photo-Fenton process under UVC irradiation. *J. Environ. Manag.* **2021**, *283*, 111987. [CrossRef] [PubMed]
32. Thabet, R.H.; Fouad, M.K.; Sherbiny, S.A.E.; Tony, M.A. Zero-Waste Approach: Assessment of Aluminum-Based Waste as a Photocatalyst for Industrial Wastewater Treatment Ecology. *Int. J. Environ. Res.* **2022**, *16*, 36. [CrossRef]
33. Xu, Z.; Zhang, M.; Wu, J.; Liang, J.; Zhou, L.; Lǔ, B. Visible light-degradation of azo dye methyl orange using TiO_2/β-FeOOH as a heterogeneous photo-Fenton-like catalyst. *Water Sci. Technol.* **2013**, *68*, 2178–2185. [CrossRef] [PubMed]
34. Soliman, E.M.; Ahmed, S.A.; Fadl, A.A. Adsorptive removal of oil spill from sea water surface using magnetic wood sawdust as a novel nano-composite synthesized via microwave approach. *J. Environ. Health Sci. Eng.* **2020**, *18*, 79–90. [CrossRef] [PubMed]
35. Wang, S.; Long, J.; Jiang, T.; Shao, L.; Li, D.; Xie, X.; Xu, F. Magnetic Fe_3O_4/CeO_2/g-C_3N_4 composites with a visible-light response as a high efficiency Fenton photocatalyst to synergistically degrade tetracycline. *Sep. Purif. Technol.* **2021**, *278*, 119609. [CrossRef]
36. Gouda, R.; Baishya, H.; Qing, Z. Application of Mathematical Models in Drug Release Kinetics of Carbidopa and Levodopa ER Tablets. *J. Dev. Drugs.* **2017**, *6*, 1–8. [CrossRef]
37. Vummaneni, V.; Nagpal, D.; Surapaneni, S. Formulation and optimization of famotidine floating tablets using 23 factorial design. *J. Pharm. Res.* **2012**, *5*, 5280–5284.
38. Miron, S.M.; Brendlé, J.; Josien, L.; Fourcade, F.; Rojas, F.; Amrane, A.; Limousy, L. Development of a new cathode for the electro-Fenton process combining carbon felt and iron-containing organic–inorganic hybrids. *Comptes Rendus Chim.* **2019**, *22*, 238–249. [CrossRef]

39. Wang, P.; Li, L.; Pang, X.; Zhang, Y.; Zhang, Y.; Dong, W.-F.; Yan, R. Chitosan-based carbon nanoparticles as a heavy metal indicator and for wastewater treatment. *RSC Adv.* **2021**, *11*, 12015. [CrossRef]
40. Rafi, M.M.; Ahmed, K.S.Z.; Nazeer, K.P.; Kumar, D.S.; Thamilselvan, M. Synthesis, characterization and magnetic properties of hematite (aFe_2O_3) nanoparticles on polysaccharide templates and their antibacterial activity. *Appl. Nanosci.* **2015**, *5*, 515–520. [CrossRef]
41. Gonzalez, C.C.; Arriaga, J.U.N.; Garc, P.E. Physicochemical properties of chitosan–magnetite nanocomposites obtained with different pH. *Polym. Polym. Compos.* **2021**, *29*, S1009–S1016.
42. Farzana, M.H.; Meenakshi, S. Photocatalytic aptitude of titanium dioxide impregnated chitosan beads for the reduction of Cr(VI). *Int. J. Biol. Macromol.* **2015**, *72*, 1265–1271. [CrossRef] [PubMed]
43. Mirzaei, A.; Chen, Z.; Haghighat, F.; Yerushalmi, L. Removal of pharmaceuticals from water by homo/heterogonous Fenton-type processes—A review. *Chemosphere* **2017**, *174*, 665. [CrossRef] [PubMed]
44. Nithya, A.; Jothivenkatachalam, K.; Prabhu, S.; Jeganathan, K. Chitosan Based Nanocomposite Materials as Photocatalyst. *Mater. Sci. Forum* **2014**, *781*, 79. [CrossRef]
45. Neyens, E.; Baeyens, J. A review of classic Fenton's peroxidation as an advanced oxidation technique. *J. Hazard. Mater.* **2003**, *98*, 33. [CrossRef]
46. Al-Ghamdi, A.A.; Galhoum, A.A.; Alshahrie, A.; Al-Turki, Y.A.; Al-Amri, A.M.; Wageh, S. Superparamagnetic multifunctionalized chitosan nanohybrids for efficient copper Adsorption: Comparative performance, stability, and mechanism insights. *Polymers* **2023**, *15*, 1157. [CrossRef]